

SIMULATION OF HEAT EXCHANGE DURING SIMPLE SHEAR OF SHEET STEEL

ALEXIS RUSINEK*
STEFAN P. GADAJ**
WOJCIECH K. NOWACKI**
JANUSZ R. KLEPACZKO*

* *Laboratory of Physics and Mechanics of Materials (LPMM) Metz University, Metz, France*

** *Institute of Fundamental Technological Research (IPPT), Warsaw*

e-mail: wnowacki@ippt.gov.pl

An original technique to measure the temperature increase in the shear zone during quasi-static loading of a sheet metal is reported. The set-up used to perform such a test has been developed in IPPT-Warsaw (Gadaj et al., 1996). The tested material is a ES sheet steel (Enhanced Formability) used in automotive industry. In addition, several tests have been performed on this material for different strain rates ($10^{-4} \leq \dot{\gamma} \leq 10^3 \text{ s}^{-1}$) in LPMM-Metz (Nguyen and Nowacki, 1998; Rusinek and Klepaczko, 2001). The experimental results enabled formulation of original visco-plastic constitutive relations (Rusinek and Klepaczko, 2001). Those constitutive relations have been implemented into a numerical code to simulate the experimental results and to compare the temperature gradient in the shear band and to calibrate the heat conduction into the surface contact (specimen-grips). The comparison between the experimental and numerical results yielded complete agreement. Thus, the visco-plastic model implemented in this study is well defined for this type of problem. Moreover, the numerical simulations indicated that at a high strain rate, $\dot{\gamma} \approx 10^3 \text{ s}^{-1}$, the heat evacuation to the surface contact of the grips seemed to be negligible. In that case the specimen was thermally isolated and the temperature increase took place essentially within the shear zone.

Key words: shear test, sheet metal, infrared thermography, visco-plastic behavior, numerical simulation

1. Introduction

Simulation of a construction response during different loadings requires knowledge of constitutive relations which govern behaviour of the materials.

One of the most important causes of damage to thin-walled constructions is shear and buckling. Therefore, a simple shear test is very important for experimental investigation of constitutive relations. It allows studying the behaviour of solids during homogeneous plastic deformation in shear up to 90% (Gadaj et al., 1996; Nguyen and Nowacki, 1998; Rusinek and Klepaczko, 2001; Gary and Nowacki, 1994). The main progress in the investigations was application of a special device, which enables for transformation of the compression mode of loading into the shear mode.

Plastic deformation of a metal is always accompanied by production of heat. Movement of dislocations and other defects (for example dislocation pile-ups) are the main sources of heat. The heat generated causes increase of temperature and, in consequence, changes the deformation process. Simultaneously, the heat is dissipated to the surroundings. The increase of temperature in the deformed volume depends on the intensity of heat sources. The temperature increase depends on the metal kind, rate of deformation and rate of heat evacuation. For simulation of heat transfer during plastic deformation of a solid it is necessary to create an adequate mathematical model with the adequate initial and boundary conditions. It is also important to make a choice of an adequate numerical method. This enables calculation of temperature changes during such process. The measurement of temperature changes must be carried out with the help of an experimental technique, which does not disturb temperature distribution in the sample and is free from any internal effect. Employing the thermovision camera allows satisfying of those conditions. The aim of this work is to model the heat conduction, which occurs during quasi-static simple shear at low rates. As a result numerical simulation of this process is attempted and comparison of the obtained results with experimental data of the temperature fields determined by means of the thermovision camera is performed.

2. Heat conduction in a deformed metal

In real conditions plastic deformation of metals is related to heat generation and its exchange with the surroundings. During simple shear, initially the shear zones in the specimen are deformed homogeneously. It means that the heat sources are distributed homogeneously as well. Because of the large mass of grips in comparison to the mass of the specimen, and because of high heat conductivity of steel, the heat exchange between the grips and specimen occurs mainly by the heat conduction. The heat exchange intensity also depends

on the rate of deformation, because the heat conduction is limited at short time intervals. During quasi-static deformation the majority of the generated heat flows to the non-deformed part of the specimen and then to the grips. In dynamic conditions, for example at strains higher than 20 s^{-1} , plastic deformation in most of metals takes place in almost adiabatic conditions (Gadaj et al., 1996; Oussouadi and Klepaczko, 1991). In solids, in agreement with the Fourier law, the heat flux is proportional to the thermal gradient, which is defined along the direction of the heat flow

$$\mathbf{q} = -k\nabla T \quad (2.1)$$

where

- \mathbf{q} – heat flux
- ∇T – temperature gradient
- k – thermal conductivity

In the present case only the normal heat conduction to the specimen surface is assumed. Since the thermal conductivity of metals is isotropic it can be assumed as a scalar quantity.

In metals the thermal conductivity is relatively good because the heat transfer occurs mainly by the movement of free electrons. The temperature field in a solid is described by the following differential equation

$$k\nabla^2 T + q_s = \rho C_p \frac{\partial T}{\partial t} \quad (2.2)$$

where

- ∇^2 – Laplace operator, $\nabla^2 = \frac{\partial^2}{\partial x_1^2} + \frac{\partial^2}{\partial x_2^2} + \frac{\partial^2}{\partial x_3^2}$
- T – temperature in Kelvins
- q_s – intensity of the heat sources
- ρ – density
- C_p – specific heat at constant pressure.

Equation (2.2) defines the heat conduction in a solid being in a transient state with internal sources of heat. To solve this equation it is necessary to define the initial and boundary conditions for temperature. In most cases of metal deformation the initial temperature is assumed constant ($T_0 = \text{const}$). During simple shear, it is assumed that the heat exchange at both sides of the separation surface of the specimen grips is described by Fourier's law, and the temperature at the separation surfaces of both parts (specimen and grip) is the same

$$T_p = T_u \quad (2.3)$$

where

- T_p – temperature of the specimen
 T_u – temperature of the grip
 q_s – capacity of the heat sources at both sides of the separation defined by Eq. (2.1).

At the same time, there is an imperfection of the thermal transfer between the surfaces in contact, caused by imperfect contact of those surfaces. The gaps between the surfaces in contact are usually filled with a gas (air), which has a less thermal conductivity in comparison to the contacted metals. This contact imperfection is a function of many factors and is very difficult to estimate. Usually, it is taken into account by introduction of an equivalent surface conductivity.

3. Experimental investigations

The tested steel sheets are used in automotive industry. The ES steel has the following composition (wt %): C – 0.02%; Mn – 0.2%; S – 0.01%; P – 0.006%; Al. – 0.04%. Its mean grain size is $8.6 \mu\text{m}$ (BCC structure), cf. Fig. 1.

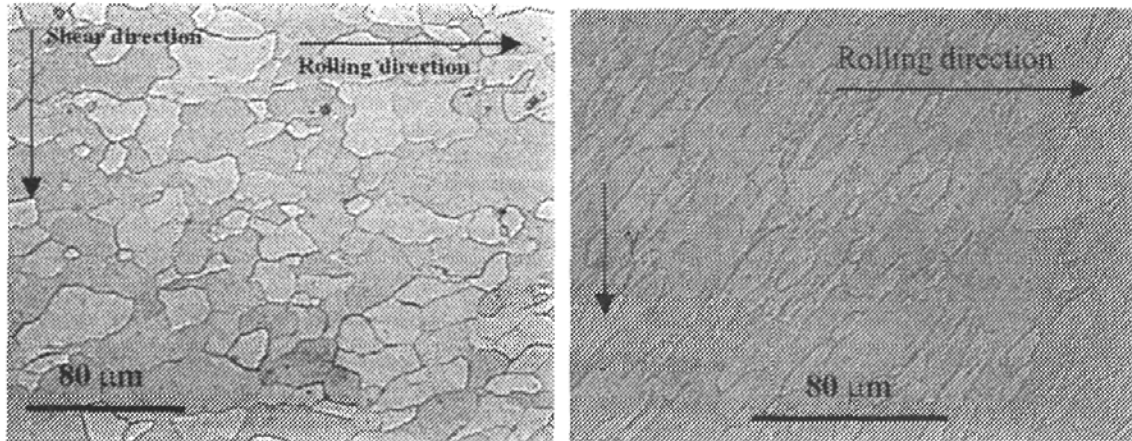


Fig. 1. Microstructure of sheet steel ES, (a) cold rolled and annealed, (b) microstructure after deformation $\gamma \approx 1$

The tests were performed on a specimen of a special shape and thickness 0.78 mm at different strain rates ($10^{-4} \leq \dot{\gamma} \leq 10^3 \text{ s}^{-1}$), Nguyen and Nowacki (1998). The first series of the tests enabled one to analyse the original viscoplastic model (Rusinek and Klepaczko, 2001). In addition, complementary experiments were performed in IPPT-Warsaw to measure the temperature

increase in the shear zones. To measure the temperature gradient in the shear zones, a strain rate of $\dot{\gamma} = 2.38 \cdot 10^{-4} \text{ s}^{-1}$) was selected and a specially designed device used in order to transform the compression loading into double shear, Fig. 2. In this device the shearing took place in two parallel shear zones in the specimen of the length of 30 mm and width of 3 mm.

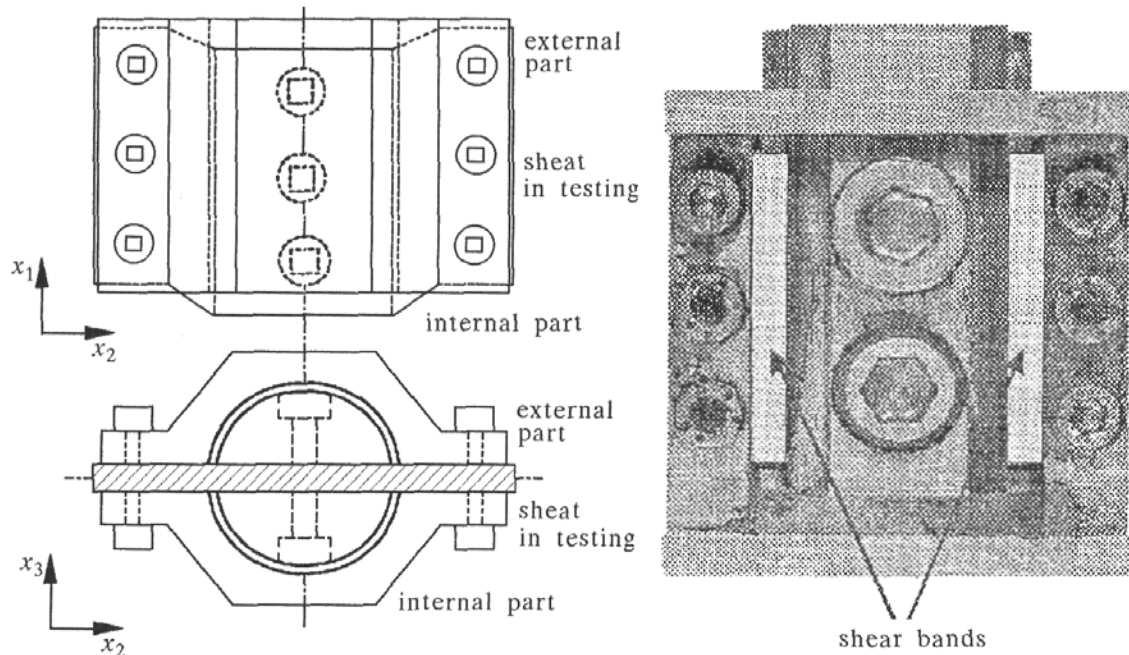


Fig. 2. Specimen geometry used in IPPT-Warsaw and a photo of the shear device (Gadaj et al., 1996)

During plastic deformation, the displacement $\delta(t)$ of the mobile central part, the force $F(t)$ and the distribution of the infrared radiation emitted by the shear bands were continuously recorded in time. The infrared radiation was measured by the thermovision camera coupled with a system of data acquisition, which allowed one to obtain thermovision pictures (thermograms). The mean-square error of temperature evaluation with this camera is about 0.1 K. In order to secure higher and more homogeneous emissivity, the surface of the shear bands was blackened with carbon powder. In Fig. 3 an example of thermogram of the shear zones, deformed with a strain rate of $\dot{\gamma} = 2.38 \cdot 10^{-4} \text{ s}^{-1}$ and a shear strain of $\gamma = 1.59$ is shown.

Since the grips are rather thick (15 mm), the thermovision camera is focused on the shear zones. The colored temperature scale is concerned only with these shear zones. Because of the large mass of the grips relative to the mass of the specimen and the high heat conductivity of steel, there is a large temperature gradient in the direction perpendicular to the shear direction.

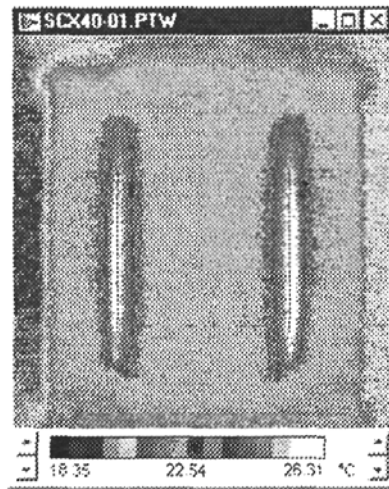


Fig. 3. Distribution of temperature during shear test

Hence, the areas of the maximum temperature are situated in the central part of the shear zones (along the direction of shear x_1 , Fig. 3). The tests make it possible to obtain relations for the shear stress versus shear strain and thermograms corresponding to variation of temperature in the shear zones at the same time. The temperature increments in the central part of the shear zones were calculated as average values of the central lines along the sheared zones, Fig. 3. Such an arrangement of the experiment enabled one to compare the mechanical behaviour $\tau(\gamma)$ and the temperature increments in the shear zones $\Delta T(\gamma)$, Fig. 4.

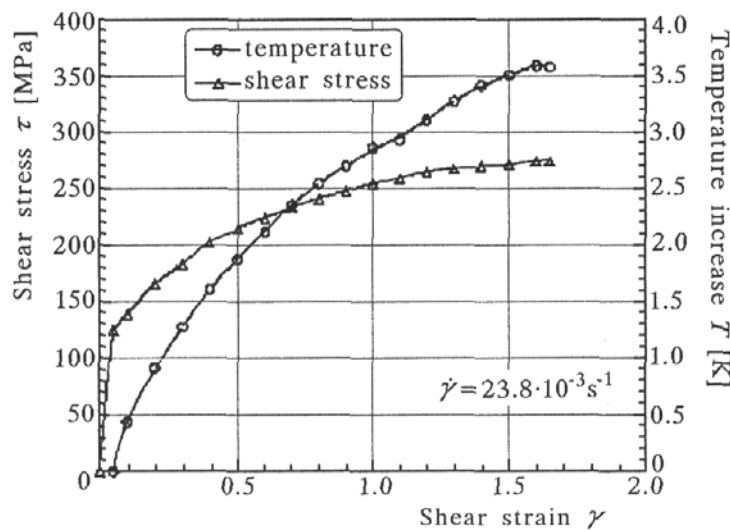


Fig. 4. Temperature and stress-strain curves, experimental results for $\dot{\gamma} = 2.38 \cdot 10^{-4} \text{ s}^{-1}$

The changes of temperature caused by the heat exchange with the grips were determined as follows. On the thermograms obtained during shearing five horizontal levels were chosen (Fig. 5) intersecting the shear zones perpendicular to the shear direction x_1 . The coordinate x_2 at the beginning of each level was the same. Along these 5 levels the distributions of the temperature ΔT were determined. For example, level 5 shows the lowest temperature increments.

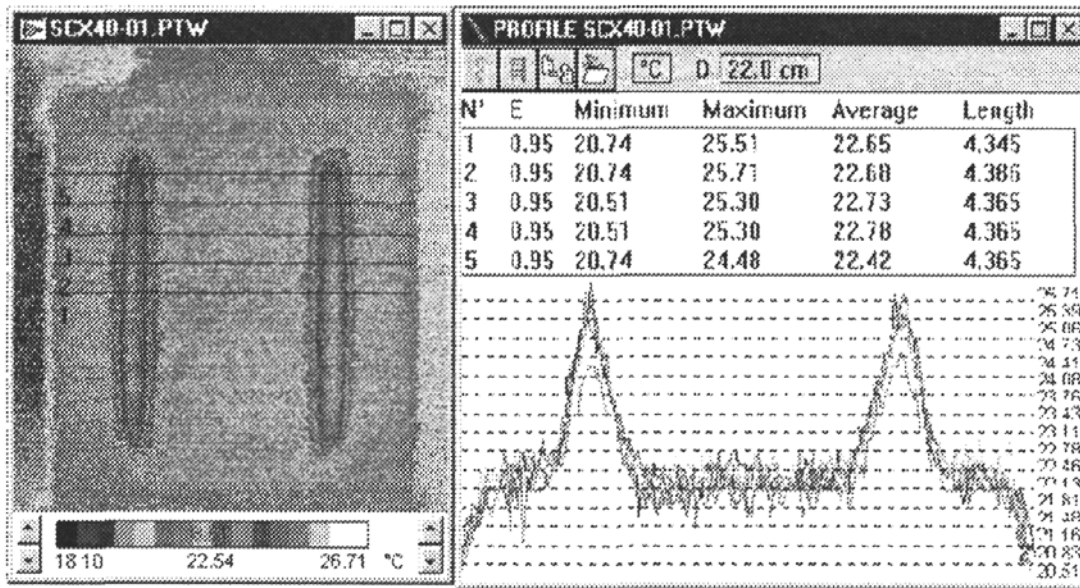


Fig. 5. Definition of the measure point along the shear zone and profile of temperature with the specimen length

For the experimental conditions ($\dot{\gamma} = 2.38 \cdot 10^{-4} \text{ s}^{-1}$, $\gamma = 1.59$) the mean temperature increase in the central part of the shear zone is approximately equal to 3.5 K. To analyse complete temperature distribution in the shear bands a numerical approach has been used. The hybrid approach confirmed on the one hand the proposed constitutive relation and enabled one to study the development of the temperature fields on the other.

4. Theoretical analysis of simple shear

The following relations define simple shear in the direction x_1 , in the coordinates shown in Fig. 2

$$\begin{aligned}
 U_1 &= \gamma(t)x_2 & V_1 &= \dot{\gamma}x_2 \\
 U_2 &= U_3 = V_2 = V_3 = 0
 \end{aligned}
 \tag{4.1}$$

where γ and $\dot{\gamma}$ are respectively the plastic shear strain and the shear strain rate. The strain tensor $\boldsymbol{\varepsilon}$ has only a non-zero component $\varepsilon_{12} = \gamma$ and the stress tensor $\boldsymbol{\sigma}$ has only the following non-zero components

$$\boldsymbol{\sigma} = \begin{bmatrix} \sigma_{11} & \tau \\ \tau & \sigma_{22} \end{bmatrix} \quad \tau = \sigma_{12}
 \tag{4.2}$$

On the basis of the experimental results obtained in LPMM-Metz in collaboration with IPPT-Warsaw (Gadaj et al., 1996), an original visco-plastic model has been derived (Rusinek and Klepaczko, 2001) to describe thermo-visco-plastic behaviour of the sheet steel ES. The constitutive relations are based on earlier works on modeling by Klepaczko (1975, 1987). Although the model is phenomenological, it is based, to some extent, on physical considerations. It is assumed that the shear stress τ is a function of the shear strain γ , the shear strain rate $\dot{\gamma}$ and the temperature T

$$\tau = f(\gamma, \dot{\gamma}, T)
 \tag{4.3}$$

In fact, it is very important to take into account the strain rate and temperature sensitivity of the flow stress as the hardening of a material is directly related to these parameters. Thus, the increment of the flow stress is written as

$$d\tau = \left. \frac{\partial \tau}{\partial \gamma} \right|_{\dot{\gamma}, T} d\gamma + \left. \frac{\partial \tau}{\partial \dot{\gamma}} \right|_{\gamma, T} d\dot{\gamma} + \left. \frac{\partial \tau}{\partial T} \right|_{\gamma, \dot{\gamma}} dT
 \tag{4.4}$$

During tests the strain rate is constant and it is imposed as a control parameter. In this case, the previous relation is reduced to

$$d\tau = \left. \frac{\partial \tau}{\partial \gamma} \right|_{\dot{\gamma}, T} d\gamma + \left. \frac{\partial \tau}{\partial T} \right|_{\gamma, \dot{\gamma}} dT \quad \text{with } \dot{\gamma} = \text{const}
 \tag{4.5}$$

Using the definition of the strain hardening coefficient $n = \partial \tau / \partial \gamma$, it is possible to define the hardening coefficient in adiabatic conditions n_{ad} in comparison with isothermal conditions n_{is}

$$n_{ad} = n_{is} + \nu \frac{\beta}{\rho C_p} \tau_{is}
 \tag{4.6}$$

where ν is the temperature sensitivity (negative) and β is the coefficient of stored energy (Oliferuk et al., 1985).

With this relation the effect of temperature on the flow stress can be studied and analysed. Thus, the temperature increase has a substantial effect on the flow stress and it induces a decrease in the shear stress with plastic strain. The thermo-visco-plastic relation, which takes into account strain hardening, strain rate sensitivity and thermal softening effect is used. The total shear stress τ is a sum of two components τ_μ and τ^* which are respectively the internal and the effective stress. The first component is directly related to the strain hardening and the second one defines the contribution due to thermal activation (combination of temperature and strain rate). Thus, the shear stress is written as

$$\tau(\gamma, \dot{\gamma}, T) = \frac{\mu(T)}{\mu_0} [\tau_\mu(\gamma, \dot{\gamma}, T) + \tau^*(\dot{\gamma}, T)] \quad (4.7)$$

where μ_0 is the shear modulus at $T = 0$ K and $\mu(T)$ is the evolution of the shear modulus as a function of temperature – this expression is based, to some extent, on physical considerations (Klepaczko, 1975). The explicit expression for relative changes of the shear modulus is the following

$$\frac{\mu(T)}{\mu_0} = 1 - \frac{T}{T_m} \exp\left[\theta^* \left(1 - \frac{T_m}{T}\right)\right] \quad (4.8)$$

where T_m is the melting temperature and $\theta^* = T^*/T_m$, with T^* being the characteristic temperature.

This formulation allows one to find correct temperature approximation of the shear modulus of different steels, Fig. 6.

The final expressions for both stress components are the following

$$\tau_\mu(\gamma, \dot{\gamma}, T) = B(\dot{\gamma}, T)(\gamma_0 + \gamma)^{n(\dot{\gamma}, T)} \quad (4.9)$$

where $B(\dot{\gamma}, T)$ and $n(\dot{\gamma}, T)$ are respectively the modulus of plasticity (discussed later) and the strain hardening coefficient. The explicit form for the second component (effective stress) in Eq. (4.7) is

$$\tau^*(\dot{\gamma}, T) = \tau_0^* \left[1 - D_1 \left(\frac{T}{T_m}\right) \log \frac{\dot{\gamma}^{max}}{\dot{\gamma}}\right]^{m^*} \quad (4.10)$$

with

$$\tau^*(\dot{\gamma}, T) \geq 0 \quad \text{and} \quad \dot{\gamma} \leq \dot{\gamma}^{max}$$

The expression used to describe the effective stress $\tau^*(\dot{\gamma}, T)$ is similar to the equation by Arrhenius (Kocks et al., 1975), which describes the kinetics of

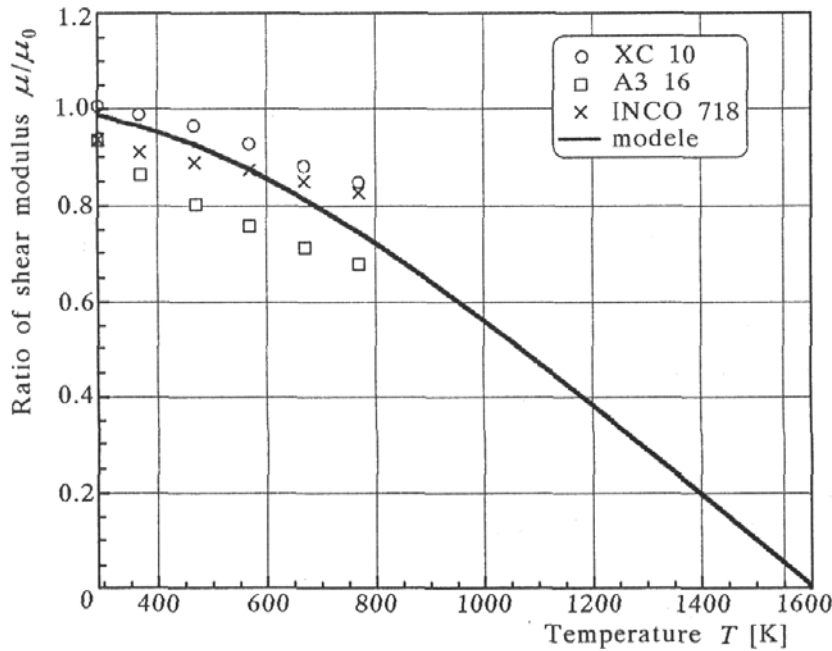


Fig. 6. Shear modulus-temperature relation, comparison between the experiment (Ben Cheikh, 1987) and analytic approach (Eq (4.9))

thermally activated processes, where τ_0^* is the effective stress at $T = 0$ K, D_1 is a constant, $\dot{\gamma}^{max}$ is the maximum strain rate of validity of the model and m^* is a coefficient which characterises the temperature and strain rate sensitivity. The effective stress $\tau^*(\dot{\gamma}, T)$ must not be negative, thus the following condition must be satisfied

$$1 - D_1 \left(\frac{T}{T_m} \right) \log \frac{\dot{\gamma}^{max}}{\dot{\gamma}} \geq 0 \quad (4.11)$$

If this condition yields a negative value then it is assumed $\tau^*(\dot{\gamma}, T) = 0$.

The strain-hardening coefficient $n(\dot{\gamma}, T)$ is defined by Eq. (4.12), which takes into account experimental observations showing that the strain hardening itself depends on temperature and strain rate, Fig. 7.

For the ES steel the strain-hardening coefficient substantially changes with temperature, particularly in adiabatic conditions (Rusinek and Klepaczko, 2001). The strain rate $\dot{\gamma}$, which corresponds to the complete adiabatic conditions is estimated as $\dot{\gamma} \approx 10^2 \text{ s}^{-1}$. For strain rates higher or equal to 10^2 s^{-1} , a significant temperature increase ΔT is observed during plastic deformation. The process of deformation is then close to the adiabatic and the flow stress is coupled with temperature. It has been found that for the strain rate $\dot{\gamma} \approx 10^2 \text{ s}^{-1}$ the coefficient of adiabatic hardening is equal to $n = 0.12$ for shear strain higher than $\gamma > 0.1$, but in isothermal conditions is equal to $n = 0.26$,

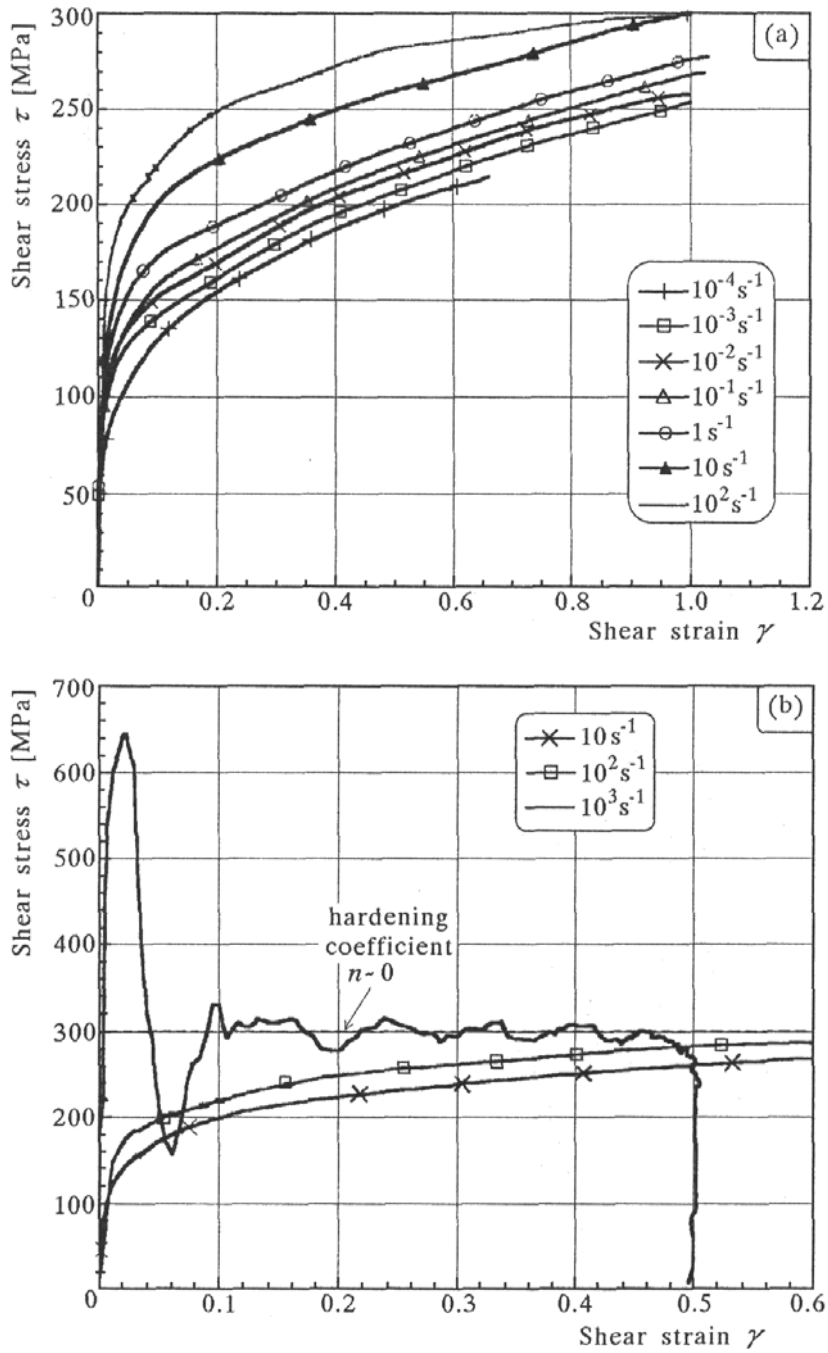


Fig. 7. Stress-strain curves at different strain rates $10^{-4} \leq \dot{\gamma} \leq 10^3$, experimental results after Oussouadi and Klepaczko (1991)

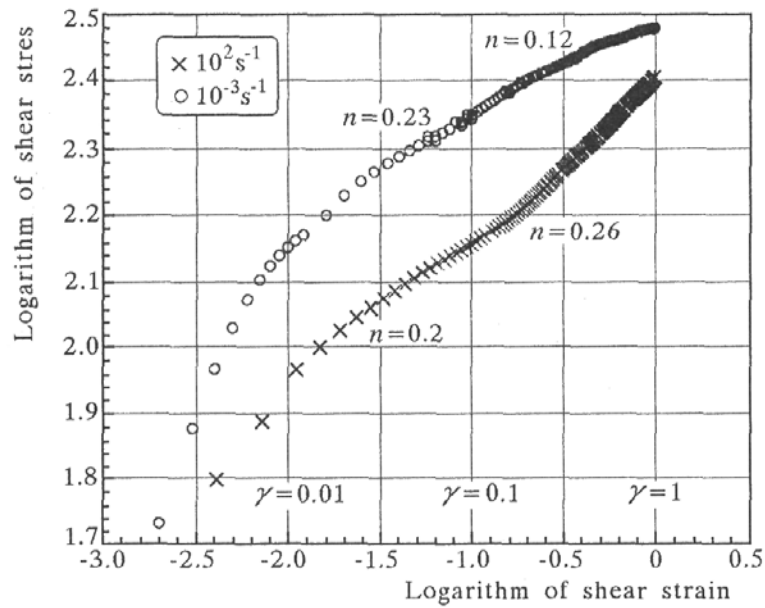


Fig. 8. Effect of adiabatic heating on the strain hardening coefficient for two different strain rates: $\dot{\gamma} = 10^{-3} \text{ s}^{-1}$ and $\dot{\gamma} = 10^2 \text{ s}^{-1}$

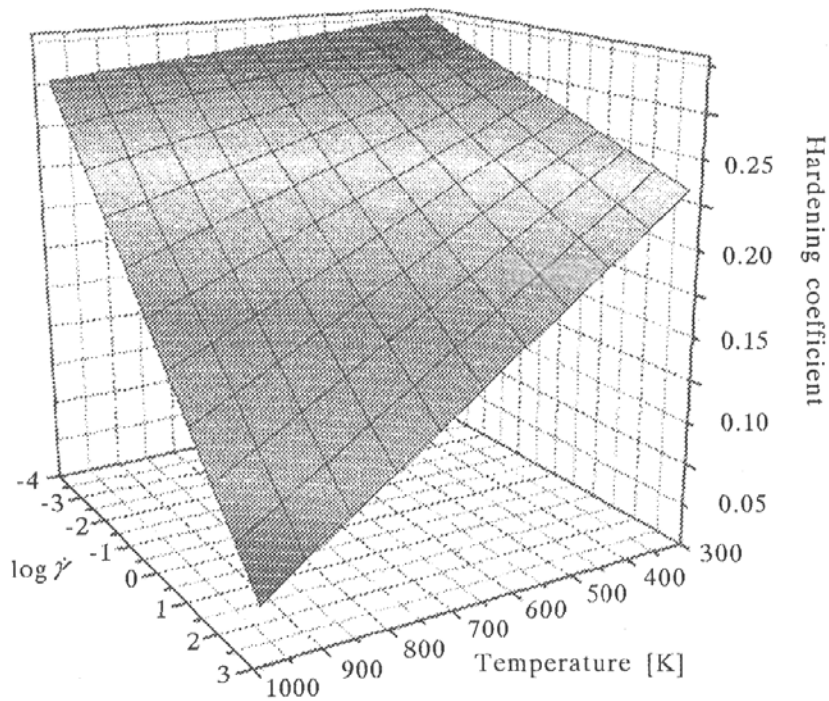


Fig. 9. Predicted changes of the strain-hardening coefficient with temperature and strain rate

Fig. 8. The strain rate of $\dot{\gamma} = 10^2 \text{ s}^{-1}$ is high enough to intensify thermal softening of the material. Thus, the expression for $n(\dot{\gamma}, T)$ is linearised in terms of the strain rate and temperature

$$n(\dot{\gamma}, T) = n_0 \left[1 - D_2 \left(\frac{T}{T_m} \right) \log \frac{\dot{\gamma}}{\dot{\gamma}^{min}} \right] \quad (4.12)$$

where n_0 and D_2 are material constants and $\dot{\gamma}^{min}$ is the minimum strain rate, which defines the quasi-static stress-strain relation. The evolution of $n(\dot{\gamma}, T)$ as a function of strain rate and temperature is shown in Fig. 9.

The strain-hardening coefficient is assumed to be equal zero if the following expression is satisfied

$$1 - D_2 \left(\frac{T}{T_m} \right) \log \frac{\dot{\gamma}}{\dot{\gamma}^{min}} < 0 \quad (4.13)$$

Moreover, to approximate the evolution of the modulus of plasticity $B(\dot{\gamma}, T)$ the following expression has been used

$$B(\dot{\gamma}, T) = B_0 \left[\left(\frac{T}{T_m} \right) \log \frac{\dot{\gamma}^{max}}{\dot{\gamma}} \right]^{-\nu} \quad (4.14)$$

where B_0 is the material constant and ν is the temperature sensitivity.

The formula for B , Eq. (4.14), is a function of the homologous temperature modified by strain rate (MacGregor and Fisser, 1988). The comparison between the experimental results and the constitutive relation is shown in Fig. 10 for strain rates varying from $10^{-4} \leq \dot{\gamma} \leq 10^3 \text{ s}^{-1}$.

In the adiabatic conditions ($\dot{\gamma} \geq 10^2 \text{ s}^{-1}$), all quantities, which depend on temperature, are coupled via relation which describes the plastic work converted into heat

$$\Delta T_{ad} = \frac{\beta}{\rho C_p} \int_0^\gamma \tau(\xi, \dot{\gamma}, T) d\xi \quad (4.15)$$

where β is the Taylor-Quinney coefficient of stored energy (Oliferuk et al., 1985).

The adiabatic increase of temperature triggers the thermal softening phenomenon and reduces the rate of strain hardening. With the new boundary conditions (γ_{i+1} , $T_{i+1} = T_i + \Delta T$), it is possible to calculate the new shear stress τ_{i+1} in the adiabatic conditions.

In order to verify the visco-plastic model at different strain rates and temperatures a series of numerical simulations have been performed with ABAQUS Standard [11]. The aim was to simulate the shear test and to estimate

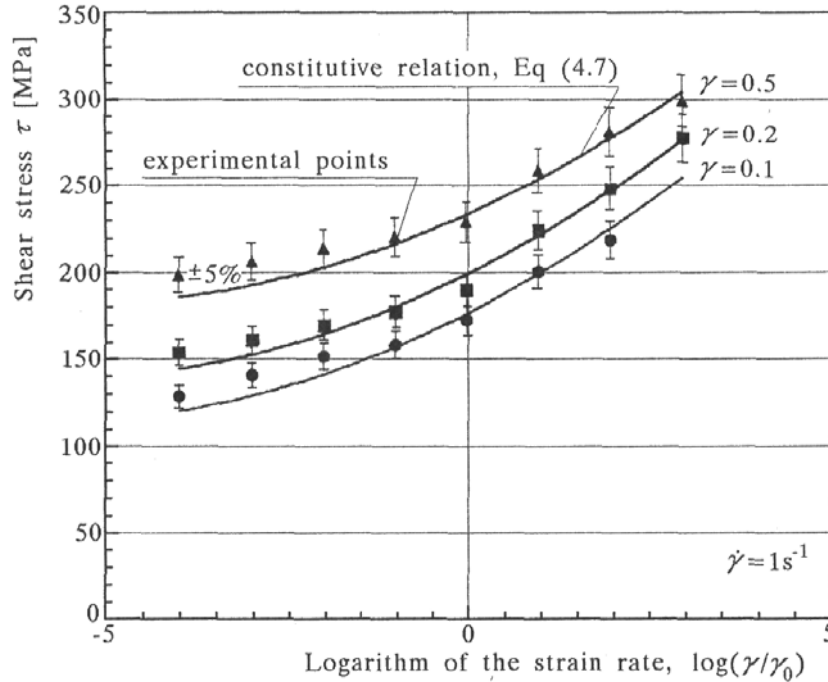


Fig. 10. Shear stress-logarithm of strain rate for different level of strain (Oussouadi and Klepaczko, 1991)

the temperature gradients in the shear zones under quasi-static loading. The final task was to compare the numerical strain and temperature distribution with the experimental results.

5. Numerical simulations

In this part of the paper description of the numerical study is discussed in details. The following boundary conditions have been assumed, see Fig. 11, with the element CPS4R, [11], and the mesh density of 10×100 elements in the shear zone. To model the grips M3D8 elements have been used, [11]. To approximate behaviour of the sheet metal the constitutive relations described previously have been used with the Huber-Mises-Hencky yield condition $f(J_2)$, where the equivalent stress σ_e is a function of the stress deviator \mathbf{S}

$$f(J_2) = \sqrt{\frac{1}{2} \mathbf{S} : \mathbf{S}} - \sigma_e(\varepsilon, \dot{\varepsilon}, T) \quad (5.1)$$

with

$$\sigma_e(\varepsilon, \dot{\varepsilon}, T) = \frac{E(T)}{E_0} [\sigma_\mu(\varepsilon, \dot{\varepsilon}, T) + \sigma^*(\dot{\varepsilon}, T)] \quad (5.2)$$

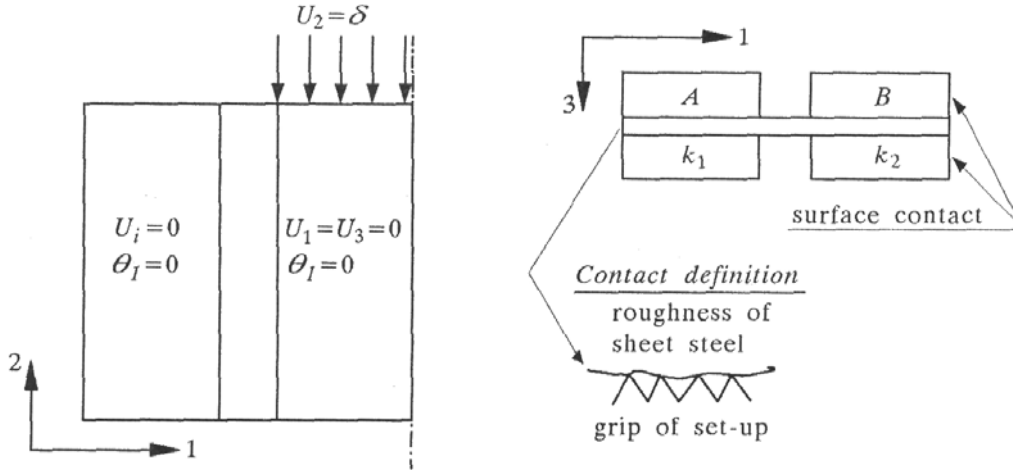


Fig. 11. Boundary conditions and definition of the coefficient of conductivity

Among several thermal conductivity coefficients k_i , two have been used to approximate correctly the heat transfer to the surface contact between the specimen and the grips ($i = 1, 2$). The effective contact in this zone is very difficult to estimate since the surface contact is not plane and regular. The surface contacts S_A and S_B are different and are respectively equal to 240 mm^2 and 600 mm^2 . The ratio between the two surface contacts is $R_s = S_B/S_A = 2.5$.

At first, calibration of the heat evacuation has been performed, in order to find the coefficients k_i . These coefficients are very important since they describe the surface conductivity of the contact by the following relation

$$k \frac{\partial^2 T}{\partial \mathbf{x}^2} + \beta \dot{\gamma} \tau(\gamma, \dot{\gamma}, T) = \rho C_p \frac{\partial T}{\partial t} \quad \mathbf{x} = (x_1, x_2, x_3) \quad (5.3)$$

The numerical results obtained for different values of k_i are shown in Fig. 12. For $k_i = 1.5 \text{ Wm}^{-1}\text{K}^{-1}$ the numerical results are in agreement with the experimental data. All is referred to the central point of the shear zone (zone 1, Fig. 5).

Because the temperature gradient along the specimen width is non-symmetric (experimental observation), it is assumed that $k_1 \neq k_2$. The best numerical results in comparison with the experiment have been obtained with the heat conductivity coefficients equal to $k_1 = 0.8 \text{ Wm}^{-1}\text{K}^{-1}$ and

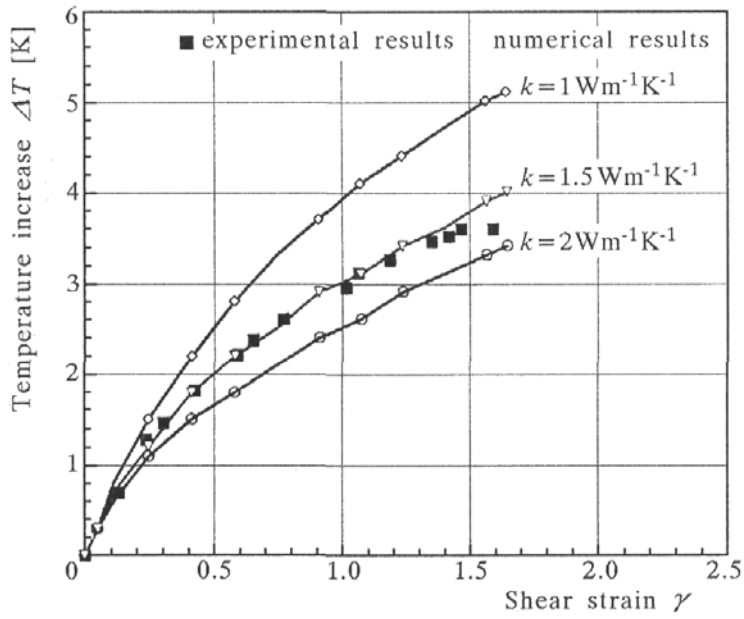


Fig. 12. Temperature-shear strain for different values of the heat conductivity coefficient, comparison between experimental and numerical results

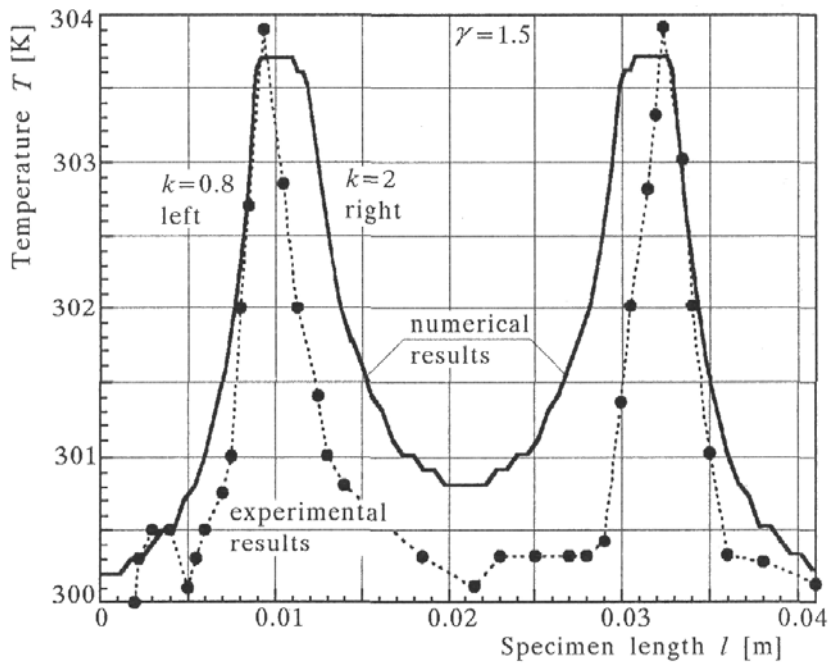


Fig. 13. Temperature distribution along the specimen width, comparison between experimental and numerical results

$k_2 = 2 \text{ Wm}^{-1}\text{K}^{-1}$, respectively for the contacts *A* and *B*. As previously assumed, the ratio of these two coefficients is the same $R_k = 2.5$. The heat conductivity inside the specimen $k = 52 \text{ Wm}^{-1}\text{K}^{-1}$ has been used during all FE simulations. The numerical results obtained with those boundary conditions and the coefficients given above are shown in Fig. 13.

Within the range of temperature of interest, that is from 293 K up to 600 K, a good approximation of temperature changes in the thermal conductivity k is assumption that k is constant (Powell and Childs, 1972).

In the case of a mild steel the temperature change of k does not exceed several percent in the above mentioned range of temperature (Powell and Childs, 1972). When the temperature range is broader, especially below the room temperature, the variation of k must be taken into consideration in all numerical analyses. In the range of higher temperatures k has a tendency to stabilise itself (Powell and Childs, 1972).

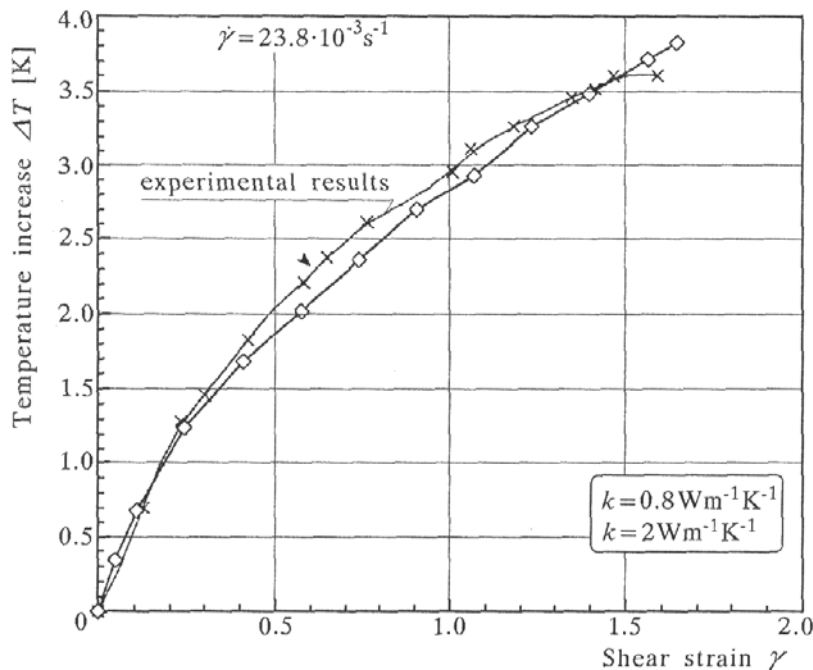


Fig. 14. Temperature-shear strain for different intensities of the heat conductivity coefficient between the interface, comparison between experimental and numerical results

The same analysis can be performed concerning the temperature increase with the shear strain in the central part of the specimen. In this case, the results are shown in Fig. 14. The coefficients that have been found via the numerical analysis allow one to assume that the heat transfer to the surface contacts is negligible, at least at higher strain rates. The type of contact at

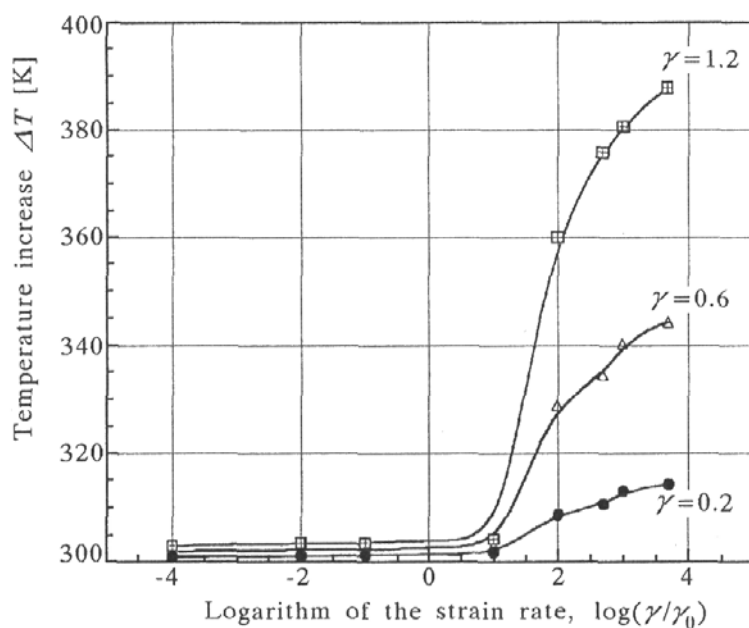


Fig. 15. Temperature increment as a function of the nominal strain rate at different levels of strain, $\gamma = 0.2, 0.6$ and 1.2

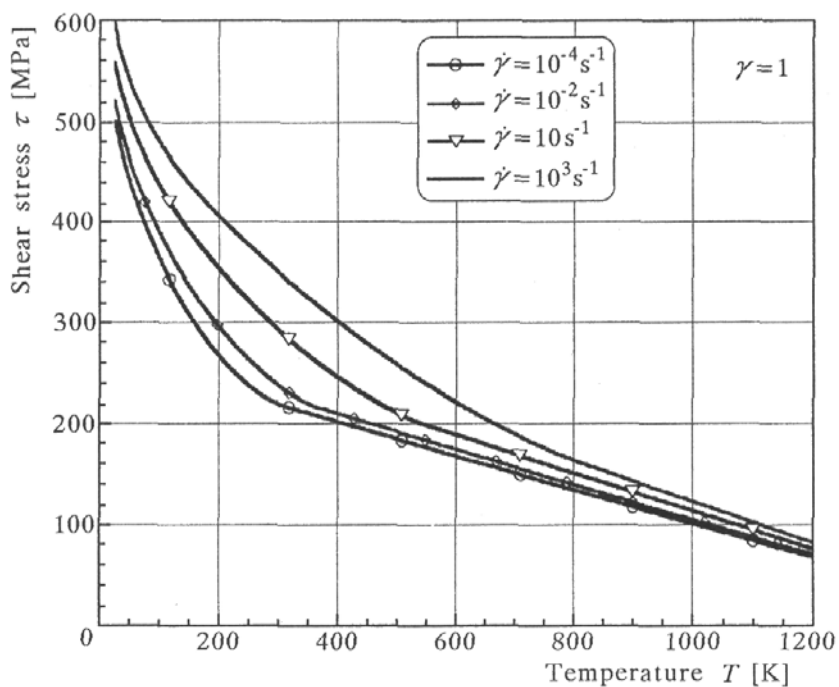


Fig. 16. Calculated stress-temperature relation for different strain rates and at strain $\gamma = 1$

these interfaces causes such a situation. Additional numerical simulations at high strain rates (adiabatic conditions) yield some results for quasi-static loading. This numerical study reveals a local temperature increase in the shear zone with increased nominal strain rates at different levels of strain. The numerical results are shown in Fig. 15. In this figure it is shown that the temperature increase is very important for the strain rate equal to or higher than 10 s^{-1} . This phenomenon intensifies with plastic strain. Thus, for the strain rate of 102 s^{-1} the temperature increase reaches 60 K. In this case the plastic behaviour of the shear zones substantially changes, which is caused by the thermal softening. It is then necessary to take into account the temperature effect, which induces a decrease of the hardening coefficient and the yield stress. The thermal softening as predicted by the constitutive relation, is shown in Fig. 16.

The knowledge of the temperature gradient created during processes of plastic deformation is very important for correct analysis of behaviour of materials at higher strain rates. The temperature gradients may perturb the local strain and temperature fields.

6. Conclusions

In this paper two topics are discussed. The first is an experimental technique that enables measuring of the temperature increase in the shear zone at different rates. At higher strain rates the temperature increase is an important factor that sometimes induce substantial changes of the strain-hardening coefficient. Moreover, the specimen design allows one to obtain a homogeneous distribution of the shear stress and shear strain within the shear zone (Klepaczko et al., 1999). In addition, an original thermo-visco-plastic model has been applied (Rusinek and Klepaczko, 2001), which allows one to predict correctly the behaviour of the ES sheet steel for different strain rates varying from 10^{-4} s^{-1} up to 10^3 s^{-1} . The analysis has shown changes in the process of the heat transfer to the specimen-grip interface by numerical simulations at different strain rates. It has been shown that the heat transfer in the grips at low strain rates (quasi-static shearing) is negligible. The negligible heat transfer is the result of the grip design where the contact is imperfect. The heat conduction coefficient determined numerically is an approximation of the heat transfer, which is the average of all heat points of the contact between the specimen and grips. Such an approach has allowed one to study the transition from quasi-isothermal to adiabatic conditions of deformation as the nominal strain rate increases.

Acknowledgements

This paper is partially supported by the State Committee for Scientific Research, KBN Project No. 7 T07 A01116 on "Localisation of deformations in shear and tension of steel sheets". First Author - A.R., acknowledges invitation to IPPT in May 2001 in the frame of the Center of Excellence AMAS. Partial support of CNRS-France is also acknowledged.

References

1. Anon. ABAQUS Manual, 1995, Version 5.6, Hibbit, Karlson and Sorensen Inc., Providence, RI, USA
2. BEN CHEIKH A., 1987, Elastoviscoplasticité a température variable, Ph.D. Paris VI
3. GADAJ S.P., NOWACKI W.K., PIECZYSKA E.A., 1996, Changes of temperature during the simple shear test of stainless steel, *Arch. Mech.*, **48**, 779-788
4. GARY G., NOWACKI W.K., 1994, Essai de cisaillement plan appliqué a des tôles minces, *J. de Phys. IV*, Coll. C8, 4
5. KLEPACZKO J.R., 1975, Thermally activated flow and strain rate history effects for some polycrystalline FCC metals, *Materials Sci. and Engng.*, **18**, 121-135
6. KLEPACZKO J.R., 1987, A practical stress-strain-strain rate-temperature constitutive relations of the power form, *J. Mech. Working Technology*, **15**, 25-39
7. KLEPACZKO J.R., NGUYEN H.V., NOWACKI W.K., 1999, Quasi-static and dynamic shearing of sheet metals, *Eur. J. Mech.*, **18**, 271-289
8. KOCKS U.F., ARGON A.S., ASHBY M.F., 1975, *Thermodynamics and Kinetics of Slip*, Pergamon Press, pp. 121-125
9. MACGREGOR C., FISSHER J.C., 1988, A velocity-modified temperature for the plastic flow of metals, *J. Appl. Mech.*, **13**, 11-16
10. NGUYEN H.V, NOWACKI W.K., 1998, Localization of thermo-elastoplastic deformation in the case of simple shear, *J. of Thermal Stresses*, **21**, 341-357
11. OLIFERUK W., GADAJ S.P., GRABSKI M., 1985, Energy storage during the tensile deformation of armco iron and austenitic steel, *Mater. Sci. Eng.*, **70**, 131-141
12. OUSSOUADI O., KLEPACZKO J.R., 1991, Analyse de la transition entre les deformations isothermes et adiabatiques dans le cas de la torsion d'un tube, *J. de Phys. III*, Coll. C3, 323-330

13. POWELL R.L., CHILDS G.E., 1972, *Thermal Conductivity*, American Institute of Physics Handbook, 3rd Ed., Mc Graw-Hill, USA, pp. 4/144-4/162
14. RUSINEK A., KLEPACZKO J.R., 2001, A double shear testing of a sheet steel at low and high strain rate in large deformation and a constitutive relation on the strain rate and temperature dependence of the flow stress, *Int. J. of Plasticity*, **17**, 87-115
15. RUSINEK A., KLEPACZKO J.R., 2001, Effect of adiabatic heating in some processes of plastic deformation, *ISIE/4*, Kumamoto, Japan, *Impact Engineering and Applications*, Elsevier Science, 541-546

Symulacja wymiany ciepła w prostym ścinaniu blach stalowych

Streszczenie

Przedstawiono oryginalną technikę pomiaru przyrostu temperatury w strefie ścinania w trakcie quasistatycznego obciążenia metalowych blach. Stanowisko badawcze do przeprowadzenia takich badań zostało skonstruowane w IPPT PAN w Warszawie. Badano blachy stalowe typu ES (Enhanced Formability), używane we francuskim przemyśle samochodowym. Dodatkowe badania zostały wykonane w LPMM-Metz, dla tego samego materiału dla innych prędkości deformacji, w zakresie $10^{-4} \leq \dot{\gamma} \leq 10^3 \text{ s}^{-1}$. Otrzymane wyniki badań pozwoliły na zaproponowanie oryginalnych równań konstytutywnych lepko-plastycznego zachowania się materiału. Zaimplementowano te równania konstytutywne w programie ABAQUS Standard w celu symulacji wyników doświadczalnych i porównaniu gradientu temperatury w strefie ścinania i kalibracji wymiany ciepła na granicy kontaktu próbka-uchwyt. Otrzymano zgodność wyników doświadczalnych i numerycznych. Stwierdzono, że przyjęty model lepko-plastyczny jest przydatny w badaniach rozważanych w pracy problemów ścinania blach. Ponadto stwierdzono, na podstawie symulacji numerycznej, że dla prędkości deformacji większej od $\dot{\gamma} \approx 10^3 \text{ s}^{-1}$, przejmowanie ciepła przez uchwyty od próbki może być pomijalne. W tym przypadku próbka jest termicznie izolowana i przyrost temperatury następuje głównie w strefie ścinania.

Manuscript received October 2, 2001; accepted for print December 12, 2001